Available online at www.sciencedirect.com

ScienceDirect

Ceramics International 39 (2013) 9099–9107

CERAMICS INTERNATIONAL

www.elsevier.com/locate/ceramint

Experimental fatigue lifetime of coated and uncoated aluminum alloy under isothermal and thermo-mechanical loadings

M. Azadi[a,b], G.H. Farrahi[a,*], G. Winter[c], W. Eichlseder[c]

[a]School of Mechanical Engineering, Sharif University of Technology, Tehran, Iran
[b]Fatigue and Wear Workgroup, Irankhodro Powertrain Company (IPCo.), Tehran, Iran
[c]Chair of Mechanical Engineering, University of Leoben, Leoben, Austria

Received 26 March 2013; received in revised form 30 April 2013; accepted 2 May 2013
Available online 15 May 2013

Abstract

This paper presents the fatigue lifetime of an aluminum–silicon–magnesium alloy, widely used in diesel engine cylinder heads, both with and without a thermal barrier coating (TBC) system. The coating system in this study consists of two layers including a 150 μm thick metallic bond coat and a zirconium oxide top coat 350 μm thick. These coating layers were applied on the substrate of A356.0 alloy by air plasma thermal spraying. The isothermal fatigue tests were conducted in low cycle fatigue (LCF) regime at various temperatures. Out-of-phase thermo-mechanical fatigue (OP-TMF) tests were also performed at different maximum temperatures and constraint factors. Experimental results demonstrate that at high temperature the coating increases the LCF lifetime of A356.0 alloy at higher strain amplitude and decreases it at lower strain amplitude. At LCF situation, thicker coating has more detrimental effect. However, the coating increases significantly the OP-TMF lifetime. To analyze the failure mechanisms, the fracture surfaces of specimens were investigated by scanning electron microscopy. The fractography of surfaces showed that the failure mechanism of TBC system in coated A356.0 alloy was separations of coating layers in the interface of the substrate and the bond coat layer. This was observed on both high temperature LCF and OP-TMF conditions.

Keywords: Aluminum alloy; Cylinder head; Low cycle fatigue; Thermo-mechanical fatigue; Thermal barrier coating

1. Introduction

Thermal barrier coating (TBC) systems can be applied to diesel engine components in order to increase the fatigue lifetime as well as enhancing the thermal efficiency. It will also reduce the fuel consumption and level of pollution [1–5]. Although this technology has been widely used in gas turbines, TBC systems were not previously used in the manufacture of diesel engines. Scientists are now actively studying the possibility of applying TBC system to the combustion chamber. A common type of TBC system is yttria stabilized zirconia (YSZ). This coating is applied by thermal spraying method as a top coat (TC) layer on the substrate where, underneath, there is usually a metallic bond coat (BC) layer Amongst papers previously presented some have dealt with the failure analysis of thermal shock test results [6] or thermal fatigue behavior [7] of TBC systems. Others have concentrated on the finite element (FE) simulation under thermal loadings [8,9] or the modeling of TBC systems under thermo-mechanical loadings when taking into account a realistic interface roughness [4,5]. It became apparent, during our survey into the literature available to us, that very little research work into the high temperature fatigue behaviors of coated aluminum alloys has been carried out. However, it is worth mentioning the following reviewed works about TBC systems on nickel-based super-alloys under thermo-mechanical fatigue (TMF) and low cycle fatigue (LCF) loadings. Wright [10] developed a TMF test including out-of-phase (OP) and in-phase (IP) conditions to determine the effect of the strain on the life of an YSZ TBC. In conclusion, he presented a power law for estimating the life based on the total mechanical strain. Failure mechanisms of TBC systems have been investigated by Tzimas et al. [11]. The TMF testing of APS and EB-PVD

*Corresponding author. Tel.: +98 21 66165533; fax: +98 21 66000021.
E-mail address: Farrahi@sharif.edu (G.H. Farrahi).

0272-8842/$ - see front matter © 2013 Elsevier Ltd and Techna Group S.r.l. All rights reserved.
http://dx.doi.org/10.1016/j.ceramint.2013.05.006

coated samples showed that both systems failed after a similar number of cycles by cracks under high mechanical strain. Cracks initiated at the interface of the BC layer, the thermally grown oxide (TGO) layer and then propagated through the BC layer to the substrate. As the mechanical strain slowed down, the cracking of the BC layer in coated system decreased and the life of the coated system increased significantly. It was also observed that there was a delamination of the TC layer. Okazaki [12] described mechanical properties and failures of super-alloys with coatings (MCrAlY where M is Fe or Co or Ni), used at hot sections of the gas turbine. TMF and LCF test results demonstrated that no clear improvement of the lifetime with coated specimens was seen under various test conditions.

Baufeld et al. [13] investigated damage mechanisms of TBC systems under IP and OP-TMF loadings. In OP-TMF tests, the cracking of the substrate was shown to control the life. While delamination cracks were observed in all samples, no spallation was observed in IP-TMF tested specimens. However, in OP-TMF tested samples, the TBC was found detached from the substrate. This detachment may have been induced by plastic deformation ahead of a fatigue crack. Otherwise it may have initiated either from the interior of the specimen or the BC layer. In another paper, Baufeld et al. [14] repeated their research for a cobalt-based super-alloy (MAR-M 509). Resulting tests showed that there were delamination cracks in the ceramic TC layer near the BC/TC interface, in particular at the BC peaks. There were also de-cohesive cracks between the BC layer and the substrate. OP-TMF tests were carried out on specimens of a nickel-based super-alloy by Peichl et al. [15]. The material was coated with a low pressure plasma spraying (LPPS) CoNiCrAlY bond coat and a zirconia TBC. No buckling and spallation was observed. However, a microscopic examination of the cross section of the interface between the BC/TC layers revealed small regions of de-bonding, especially in the direct area of the macro-cracks in TC and BC layers.

The morphological surface instabilities on BC surfaces of TBC systems, induced due to a typical thermo-mechanical loading, were investigated by Shi et al. [16]. The material consisted of a super-alloy which was coated with a BC layer. Experimental results of hollow circular cylindrical specimens showed that the morphological instabilities were strongly dependent on the load conditions.

Aguero et al. [17] investigated the oxidation resistance of iron aluminide coatings on ferritic steels. The coating exhibited perpendicular cracks due to the thermal expansion mismatch between the coating and the substrate. The cyclic oxidation, the creep resistance and the TMF testing of the coating at 650 °C indicated excellent performances. Results showed that the behavior of the slurry aluminide coated and uncoated specimens were quite different. At high strain ranges, coated specimens exhibited greater endurance than that of the uncoated specimens. However, the dependency of the endurance on the strain range of coated specimens was less than that of the uncoated specimens. At low strain range, uncoated specimens had greater endurance. The effect of the aluminide diffusion coating on LCF properties of a super-alloy (Rene 80) had been studied at the temperature of 871 °C by Rahmani and Nategh [18].

According to the literature review, different behaviors have been observed by scientists. Whilst some have reported an enhancement of the fatigue lifetime in TBC systems, others have noted a reduction. Also, the OP-TMF behavior compared to LCF behavior of coated aluminum–silicon–magnesium alloy has not been, until now, investigated.

Therefore, this article presents the results of high temperature fatigue behaviors of coated and uncoated aluminum alloy specimens under TMF/LCF loadings. A comparison is made between the results of coated and uncoated specimens. Fracture surfaces are examined by the scanning electron microscopy (SEM).

2. Materials and tests

The substrate is a cast aluminum–silicon–magnesium alloy (A356.0 or AlSi7Mg0.3) which is typically used in diesel engine cylinder heads. The element composition of A356.0 alloy is measured as 7.06% Si, 0.37% Mg, 0.15% Fe, 0.01% Cu, 0.02% Mn, 0.13% Ti and Al balance. The production method is a permanent mold gravity casting process. A typical TBC system consists of two layers. The coating layers include a metallic BC of Ni–Mo–Al (AMDRY-387) and an YSZ (METCO-204B-NS) TC with a typical composition of zirconia with 8% of yttria (ZrO_2–8 wt%Y_2O_3).

The coating process is performed on aluminum alloy cylindrical specimens by air plasma thermal spraying (APS). Before this process, specimens are blasted with SiC particles. The ratio of preliminary to second gases (Ar/H_2) is set to 39.4/6.6 values. More details of the coating process are depicted in Table 1. It should be mentioned that two coating parameters including the nozzle distance to the specimen surface and the feed rate of coating materials were optimized in our previous works [5,19]. The BC layer is 150 μm thick and the TC layer is 350 μm thick. Thus, the total thickness is about 500 μm. In order to investigate the effect of the coating thickness, another coating thickness of 250 μm is used.

Table 1
Conditions of the APS coating process.

General information				Nozzle distance (mm)		Feed rate (gr/min)	
Speed (rpm)	Power (kW)	Current (A)	Voltage (V)	for BC layer	for TC layer	for BC layer	for TC layer
1100	32	500	64	90	80	75	30

To compare the lifetime, compression–tension fatigue tests are accomplished under strain-controlled conditions. Two test types including LCF and TMF loadings are performed. LCF tests are carried out considering ASTM-E606 standard (a standard practice for strain-controlled fatigue testing) and TMF tests are performed according to COP-EUR22281EN procedure (a validated code-of-practice for strain-controlled thermo-mechanical fatigue testing).

In LCF tests, the temperature is constant due to isothermal conditions and the strain changes. These experiments are conducted in room temperature (RT) and high temperature (HT). In TMF tests, both the strain and the temperature change in an out-of-phase (OP) condition. The OP condition means maximum temperature happens at compressive loads and minimum temperature happens at tensile loads. It should be mentioned that the strain is measured by a high temperature extensometer device. The temperature is measured by K-type thermocouples in the substrate and on coating surfaces. The dimension of TMF/LCF test specimens and the location of coating layers are shown in Fig. 1.

In RT- and HT-LCF tests, the mechanical strain amplitude is set to 0.2–0.4% with a constant strain rate of 60%/min. In these experiments, the temperature is also constant but changes in each test as 25, 200 and 250 °C. In OP-TMF tests, the thermo-mechanical loading factor or the constraint factor (K_{TM}) which is defined as the ratio of the mechanical strain to the thermal strain, changes from 75% to 150%. In these tests, first the thermal strain at a zero-stress test is measured. Then, the mechanical strain is controlled at a constant K_{TM} factor. Minimum temperature is set to 50 °C and maximum temperature varies between 225 and 300 °C without any dwell times. Also, the heating/cooling rate is set to 10 °C/s. A typical loading history in TMF/LCF tests is shown in Fig. 2.

This OP type of loadings is considered due to start-stop cycles in engines. When the engine is working at high temperatures, the cylinder head is compressed by the combustion pressure and

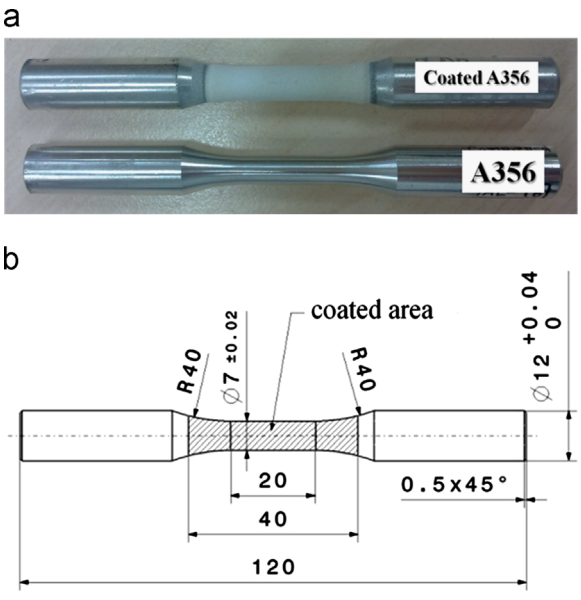

Fig. 1. Dimension of TMF/LCF test specimens and the location of coating.

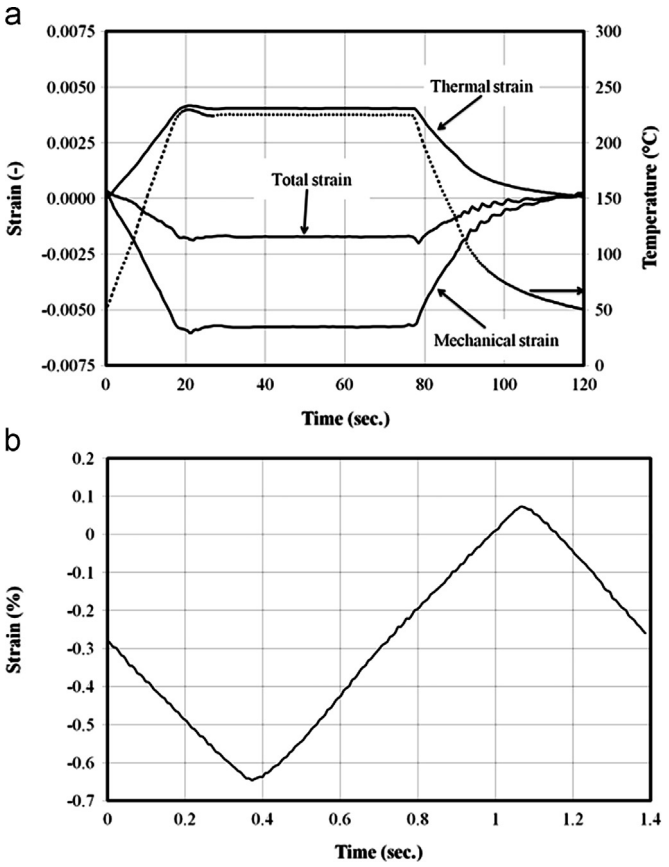

Fig. 2. Typical loading history in (a) OP-TMF tests and (b) LCF tests.

when the engine is stopped, cylinder head bolts lead to tensile stresses in the combustion chamber. Also, the range of the working temperature is about 200 °C in diesel engines [4,5]. This working temperature can be increased to 300 °C, when a TBC system is applied on the cylinder head. These are the reasons to consider 200–300 °C for maximum temperatures.

The heating system includes induction coils with a typical susceptor to heat up coated specimens indirectly with a radiation heat transfer. The cooling is done by a compressed air jet. Fig. 3 shows the susceptor used in OP-TMF and HT-LCF tests.

To obtain a correct function of TBC systems, the outer surface of coated specimens should be hotter than the substrate. It is impossible to generate this temperature profile in TMF tests while using the induction heating system, since this system will heat primarily the substrate [11,14].

To overcome this problem, a cylindrical susceptor is placed around the specimen. The specimen is therefore shielded from the direct induction heating system but exposed to the radiation heating due to the susceptor [11,14].

The susceptor is made of a super-alloy to resist high temperatures. The thick wall of this cylindrical shell can be designed to obtain a specified temperature difference between the substrate and coating layers. In fatigue tests, the susceptor is first heated up by copper coils in the induction system to become bright and red (shown in Fig. 3). Then, this bright shell heats up the coated specimen by the radiation heat

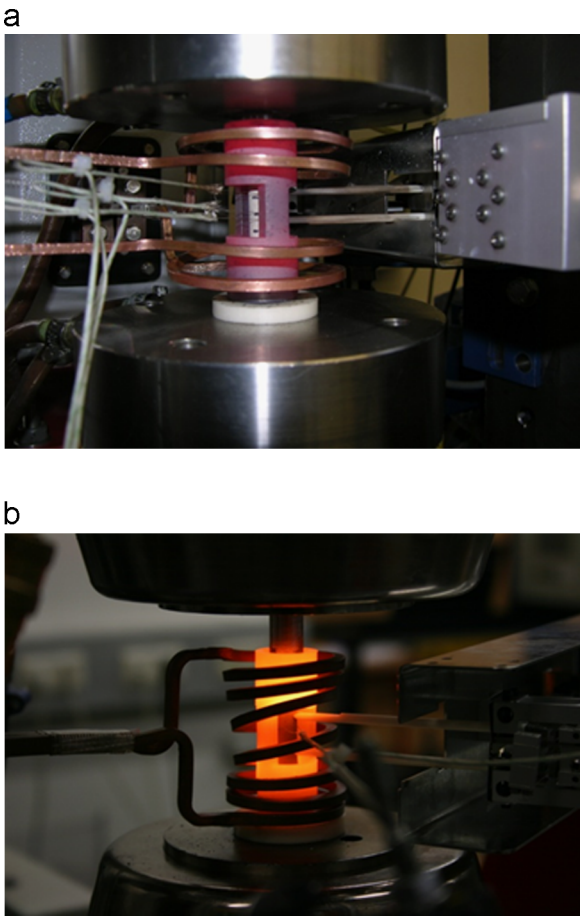

Fig. 3. Susceptor used in (a) OP-TMF tests and (b) HT-LCF tests.

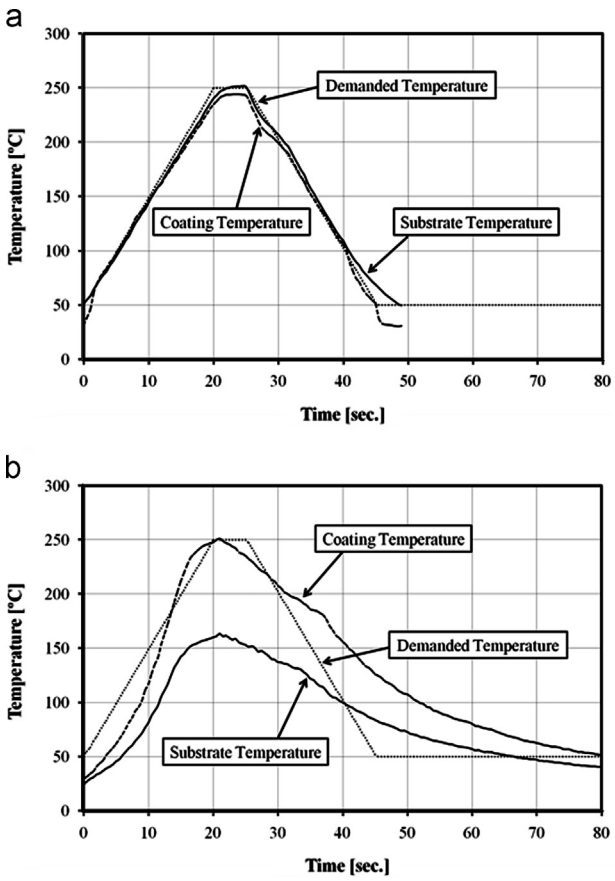

Fig. 4. Temperature distribution of coated specimens (a) without the susceptor and (b) with the susceptor.

transfer. By this method, the barrier role of coating layers will be achieved.

Fig. 4 shows the temperature distribution measured during TMF tests on coated specimens. In this figure, the results are for specimens with and without the susceptor. As illustrated, at 250 °C of maximum temperature, the temperature difference is 90 °C approximately between coating and substrate under the indirect heating condition. For a 500 μm thick coat, the temperature difference is measured almost at 110 °C and 70 °C for 300 °C and 200 °C of maximum temperature, respectively. Under the direct heating condition, the substrate temperature is more than the coating temperature. However, controlling the temperature is more difficult by using the susceptor due to the heat transfer type change from the induction to the radiation.

3. Results and discussion

The effect of using the susceptor on the HT-LCF lifetime is shown in Fig. 5 where the temperature is constant at 200 °C during the entire cycles. The result demonstrates that the fatigue lifetime is more for the indirect heating with the susceptor. The reason is due to higher plastic strain for coated specimens under the direct heating system (the induction heat) in comparison to the indirect heating system. Although, the total strain amplitude is the same for both approaches. The susceptor also increases the value of maximum stress and reduces the minimum stress in coated specimens.

Figs. 6 and 7 illustrate RT-, HT-LCF and OP-TMF results of uncoated and coated specimens, respectively. The first drop in maximum stress during cycles is considered to be the end of the lifetime in specimens.

Results show that the RT-LCF lifetime of uncoated A356.0 alloy is shorter than that one at 200 °C but longer than that one at 250 °C. This can be related to micro-structural changes in the material. Since the temperature remains constant during LCF tests, the material is aged. The yield stress and the ultimate stress of A356.0 alloy reach their maximum values at 200 °C in the ageing process. While the material goes under the over-ageing process at 250 °C [20]. This can explain the decrease of the LCF lifetime of A356.0 alloy at 250 °C and the increase at 200 °C.

Results in Fig. 6 show that the coating system increases the RT-LCF lifetime. However, at high temperature we observe two different behaviors: at higher strain amplitude, the coating system has a beneficial effect while at lower amplitude the coating system has an opposite effect. Also, under these conditions a thicker coating layer has a more detrimental effect. Fig. 7 illustrates that the coating system increases significantly the OP-TMF lifetime. Nevertheless, Fig. 7(b) shows that a 500 μm thick coat gives better lifetime and performance to the

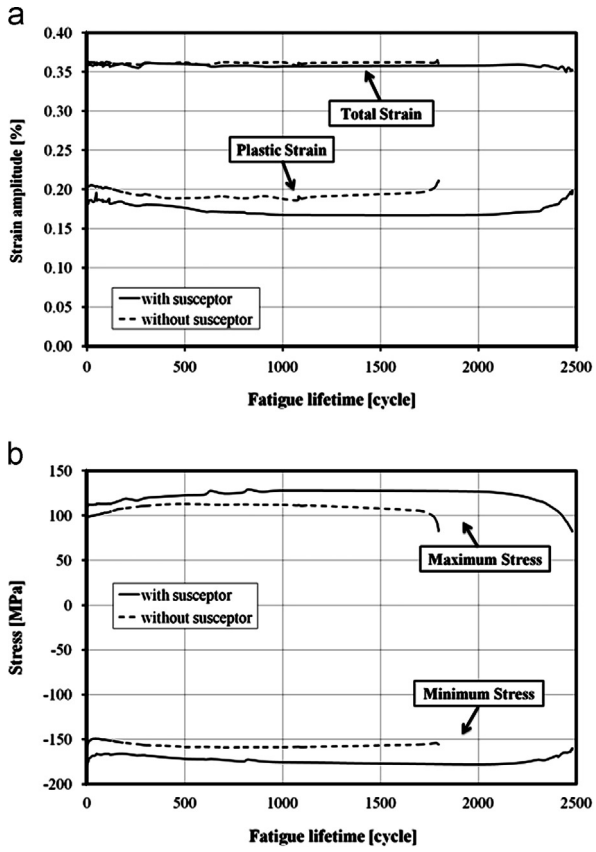

Fig. 5. HT-LCF results of coated specimens with and without the susceptor including (a) strain histories and (b) stress histories versus the fatigue lifetime at 200 °C.

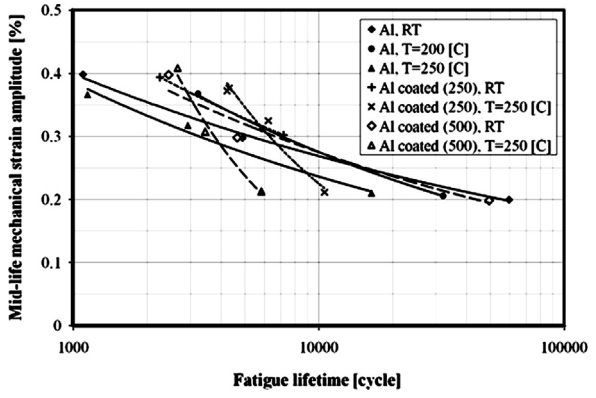

Fig. 6. The mechanical strain amplitude versus the LCF lifetime of uncoated and coated specimens.

material while a 250 μm thick coat causes a reduction of the lifetime.

Results presented in Figs. 6 and 7 provide an evidence that a 250 μm coating system gives a better LCF lifetime but a 500 μm coating system offers better TMF lifetime. This can be explained by the TBC behavior under the temperature variation. The temperature varies between maximum and minimum values in TMF tests while in LCF tests it remains constant. In TMF tests, the TBC systems protect the substrate under

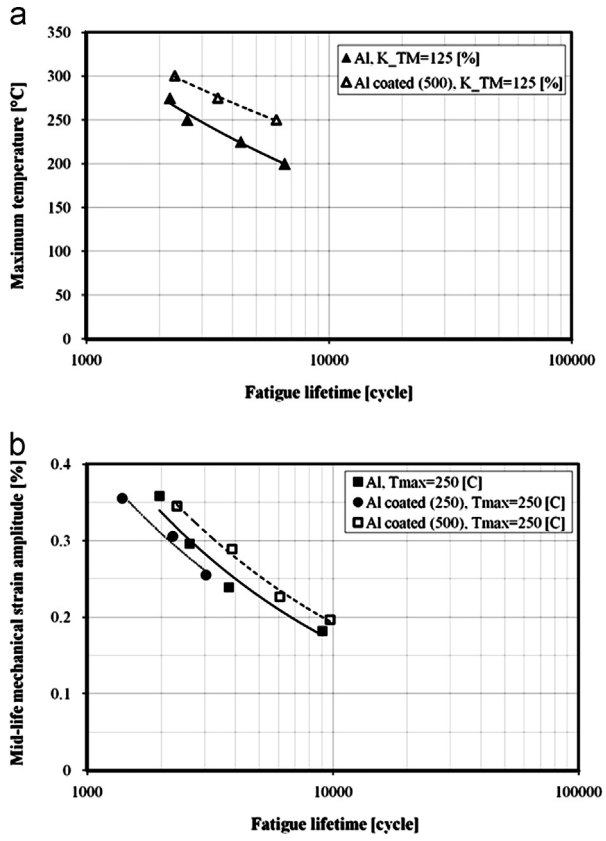

Fig. 7. The OP-TMF lifetime of uncoated and coated specimens (a) at a constant constraint factor of 125% but at various maximum temperatures and (b) at a constant maximum temperature of 250 °C but at various constraint factors.

transient thermal loadings. In LCF tests, there is no transient thermal loading and the surface temperature remains constant. Therefore, the temperature difference between coating layers and the substrate becomes less and less during the time and cycles. This can be accelerated by circumferential cracks due to high strain rates in LCF tests in comparison to TMF tests. In TMF tests, the debonding of coating layers due to transient thermal loadings has an important role in failures. Thus, a thicker coat has a better bond to the substrate. Also, the stress increases by increasing thickening the coating system [4,5] and therefore, the thinner coat has higher LCF lifetime.

As an observation in this research, the thermally grown oxide (TGO) layer is not produced since maximum temperature in TMF tests is 300 °C.

In Fig. 8(a), circumferential cracks are observed on LCF test specimens. The reason for circumferential cracks can be high mechanical loadings in LCF tests. Fig. 8(b) shows longitudinal cracks on coating surfaces of TMF test specimens. The reason for longitudinal cracks can be the substrate expansion due to transient thermal loadings. This expansion leads to a compressive radial stress in the substrate where coating layers have a constraint role. Another reason for crack types is the strain rate which is about $10^{-2}\,s^{-1}$ for LCF tests and $10^{-4}\,s^{-1}$ for TMF tests. It is widely acknowledged that the sensitivity of brittle materials, the ceramic TC layer, is high to the strain rate [21].

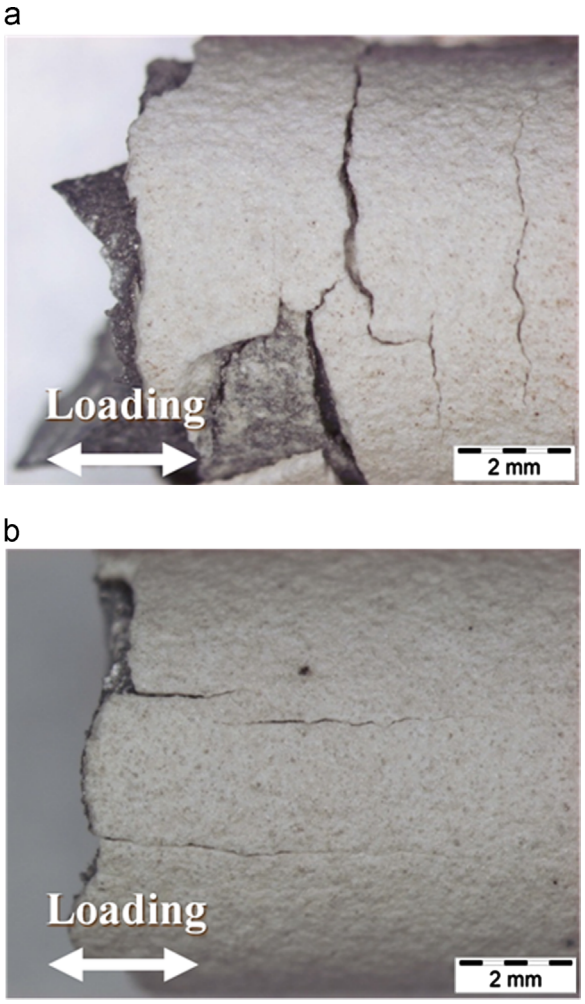

Fig. 8. Cracks on coated specimens under (a) the HT-LCF test and (b) the OP-TMF test.

To calculate analytical stresses in the elastic region, the following equations are used under steady-state conditions for given temperatures at the inner and outer walls in coated specimens [16]. The radial stress ($\sigma_r^{(i)}$) and the hoop stress ($\sigma_\theta^{(i)}$) as functions of the coated specimen radius (r) in each layer (the substrate, BC and TC layers) can be written as in the following form:

$$\sigma_r^{(i)}(r) = C_{1,i} + \frac{1}{r^2}\left(C_{2,i} - \alpha_i E_i \int_{s=a_i}^{r} T_i(s)sds\right) \quad (1)$$

$$\sigma_\theta^{(i)}(r) = C_{1,i} - \frac{1}{r^2}\left(C_{2,i} + \alpha_i E_i\left[T_i(r) - \int_{s=a_i}^{r} T_i(s)sds\right]\right) \quad (2)$$

where i is 1, 2 and 3 for the substrate, BC and TC layers, respectively. Also $\alpha_i, E_i, T_i(r)$ are the expansion coefficient, the elastic modulus and the temperature distribution in each layer. For these material properties the same values described in our previous work are used [5]. It should be mentioned that $C_{1,i}, C_{2,i}$ are constants which can calculated by boundary conditions (no pressure on both inner and outer surfaces), continuity conditions of the radial stress at interfaces and the symmetry of the tangential strain [16]. These boundary conditions are as the following:

$$\sigma_r^{(1)}(r = r_1) = \sigma_r^{(3)}(r = r_4) = 0 \quad (3)$$

$$\sigma_r^{(1)}(r = r_2) = \sigma_r^{(2)}(r = r_2) \quad (4)$$

$$\sigma_r^{(2)}(r = r_3) = \sigma_r^{(3)}(r = r_3) \quad (5)$$

$$\varepsilon_\theta^{(1)}(r = r_2) = \varepsilon_\theta^{(2)}(r = r_2) \quad (6)$$

$$\varepsilon_\theta^{(2)}(r = r_3) = \varepsilon_\theta^{(3)}(r = r_3) \quad (7)$$

where r_1, r_2, r_3 and r_4 are radius at the free surface of the substrate, the interface of the substrate/BC layer, the interface of the BC/TC layers and the free surface of the TC layer, respectively. The tangential strain ($\varepsilon_\theta^{(i)}$) is defined as the following:

$$\varepsilon_\theta^{(i)}(r) = \frac{1}{E_i}(\sigma_\theta^{(i)}(r) - \nu_i \sigma_r^{(i)}(r)) + \alpha_i T_i(r) \quad (8)$$

The results of calculating radial and hoop stresses at maximum temperature of 250 °C are demonstrated in Fig. 9. As illustrated, coating layers lead to a compressive radial stress against the expansion of the substrate. This stress produces radial cracks in TMF specimens. It is obvious that by increasing the coating thickness, the radial stress increases due to stronger constraints against the substrate expansion.

As another result, the hoop stress is maximum in the BC layer in comparison to the substrate and the TC layer.

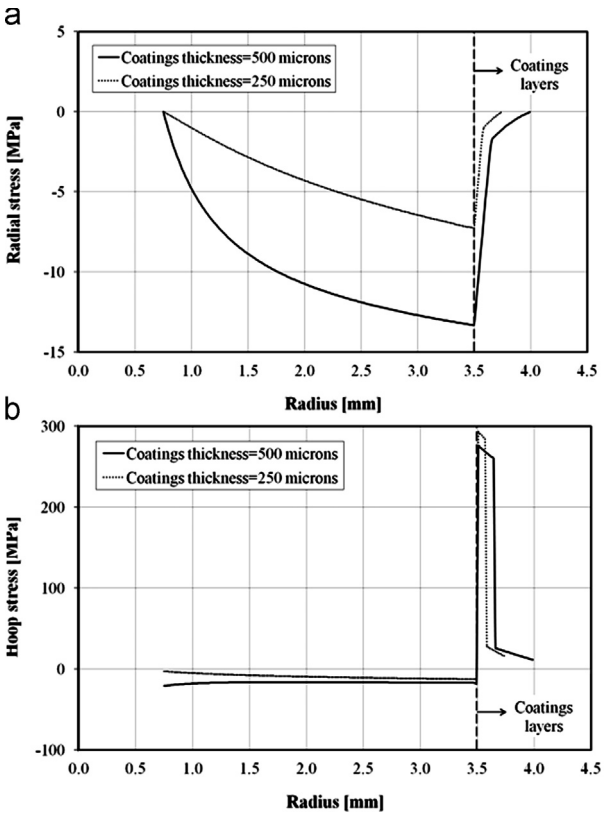

Fig. 9. (a) The radial stress and (b) the hoop stress versus the coated specimen radius at maximum temperature of 250 °C.

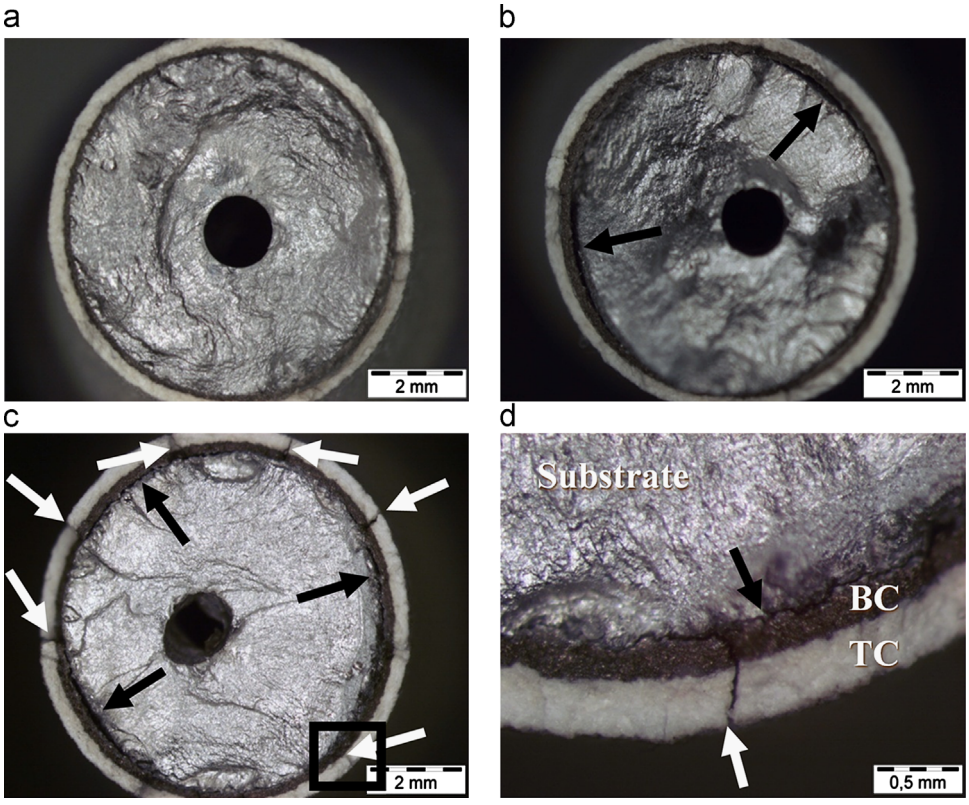

Fig. 10. The fractography of coated specimens after (a) the RT-LCF test, (b) the HT-LCF test, (c) the OP-TMF test and (d) the OP-TMF test at higher magnification.

The hoop stress of 250 μm coated specimens is less than the one in 500 μm coated specimens. This causes lower TMF lifetimes of 250 μm coated specimens in comparison to 500 μm coated specimens.

Fracture surfaces of coated and uncoated specimens are investigated after fatigue tests by the light microscopy and also the SEM.

Microscopic views of coated specimens are demonstrated in Fig. 10. In this figure, black and white arrows show cracks on coating layers and separations of coating layers at the interface of the BC layer and the substrate, respectively. As illustrated, in RT-LCF tests, no separation at interfaces is observed due to room temperature testing. For HT-LCF and OP-TMF tests, separations at the interface of the substrate and the BC layer (shown in Fig. 9 by white arrows) are observed due to the material properties mismatch. No separation is observed at the interface of BC and TC layers in high temperature fatigue tests. Cracks on coating layers are demonstrated in Fig. 10 with black arrows. SEM micrographs are also shown in Fig. 11. In this figure, black and white arrows show cracks on coating layers and separations at the interface of the BC layer and the substrate, respectively. Fracture surfaces demonstrate that there is no separation between BC and TC layers and the failure mechanism is due to cracks at interfaces of the BC layer and the substrate and also due to cracks inside the substrate. The mismatch of material properties between the BC layer and the substrate leads to a hoop stress (shown in Fig. 9) in the BC layer. The value of the yield strength for the TC layer varies from 10 to 100 MPa. The yield strength of the BC layer is equal to 270 MPa [5]. The excessive stress in the BC layer, about 300 MPa (Fig. 9), compared to other layers, can be a reason for the separation of the BC layer from the substrate as a failure mechanism in TBC systems.

4. Conclusion

In the present paper, OP-TMF, RT- and HT-LCF behaviors of coated and uncoated A356.0 alloy specimens were studied. The TBC system consists of a BC layer (Ni–Mo–Al) and a TC layer (ZrO_2–8 wt%Y_2O_3) with the total coating thickness of 250 and 500 μm.

Experimental fatigue results demonstrate that:

- The LCF lifetime of the uncoated A356.0 alloy at room temperature is shorter than that one at 200 °C but longer than that one at 250 °C. This can be related to micro-structural changes in the material.
- The fatigue lifetime is more for the indirect heating system (the radiation heat with the susceptor) in comparison to the direct heating system (the induction heat) due to higher plastic strain amplitude.
- The coating system at room temperature increases the LCF lifetime. However, at high temperature we observe two different behaviors: at higher strain amplitude, the coating system has a beneficial effect while at lower amplitude the coating system has an opposite effect.
- At the LCF situation, thicker coating system has a detri-mental effect.

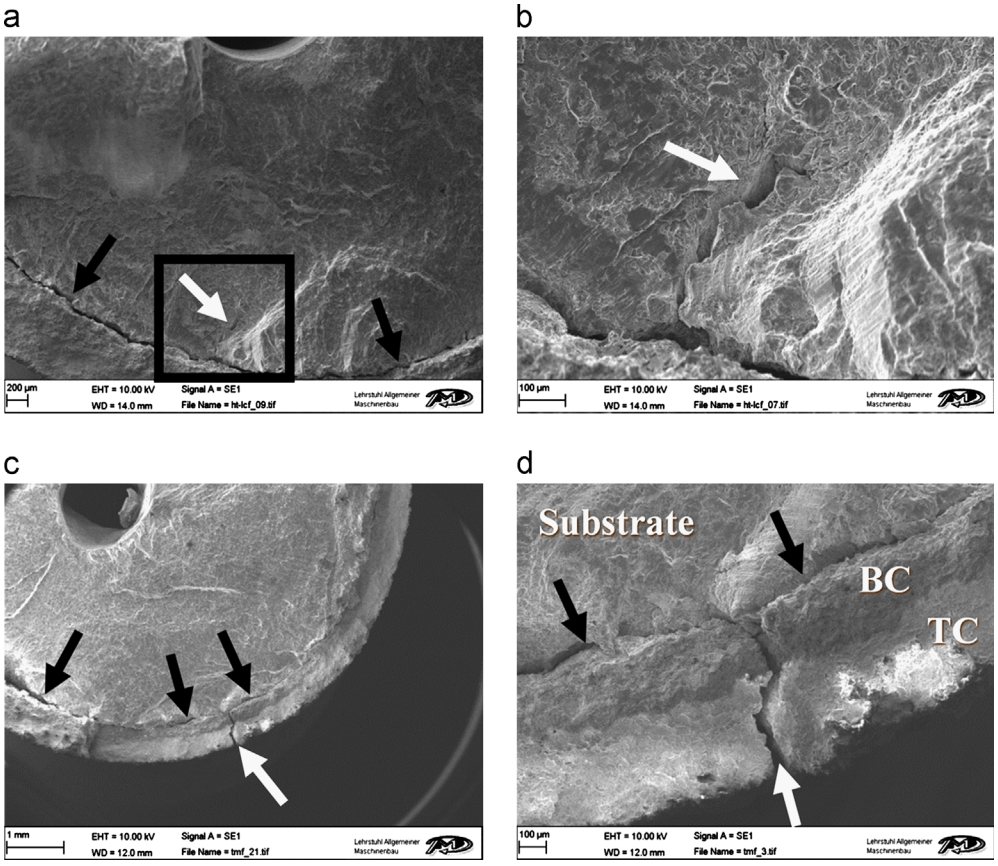

Fig. 11. SEM micrographs of coated specimens after (a) the HT-LCF test, (b) the HT-LCF test at higher magnification, (c) the OP-TMF test and (d) the OP-TMF test at higher magnification.

- The coating system increases significantly the OP-TMF lifetime. Nevertheless, a 500 μm thick coat gives better lifetime and performance to the material while a 250 μm thick coat causes a reduction of the lifetime.
- In TMF tests, the main problem is the debonding of coating layers due to transient thermal loadings and then, thicker coat has a better bond to the substrate and consequently has a better TMF lifetime.
- A 250 μm thick coat gives a better LCF lifetime whereas a 500 μm thick coat offers a better TMF lifetime. This can be explained by the TBC behavior under the temperature variation.
- The fractography of surfaces shows that the failure mechanism of TBC systems in the coated A356.0 alloy is separations of coating layers at the interface of the substrate and the BC layer. This is observed on both HT-LCF and OP-TMF conditions.

Acknowledgment

The authors thank Irankhodro Powertrain Company (IPCo.) for financial support and University of Leoben for their kind cooperation.

References

[1] T. Hejwowski, A. Weronski, The effect of thermal barrier coatings on diesel engine performance, Vacuum 65 (2002) 427–432.
[2] I. Taymaz, K. Cakir, A. Mimaroglu, Experimental study of effective efficiency in a ceramic coated diesel engine, Surface and Coatings Technology 200 (2005) 1182–1185.
[3] I. Taymaz, The effect of thermal barrier coatings on diesel engine performance, Surface and Coatings Technology 201 (2007) 5249–5252.
[4] A. Moridi, M. Azadi, G.H. Farrahi, Coating thickness and roughness effect on stress distribution of A356.0 under thermo-mechanical loadings, Procedia Engineering 10 (2011) 1372–1377.
[5] A. Moridi, M. Azadi, G.H. Farrahi, Thermo-mechanical stress analysis of thermal barrier coating system considering thickness and roughness effect, Surface and Coatings Technology http://dx.doi.org/10.1016/j.surfcoat.2012.02.019, in press.
[6] A. Bolcavage, A. Feuerstein, J. Foster, P. Moore, Thermal shock testing of thermal barrier coating—bond coat systems, Journal of Materials Engineering and Performance 13 (4) (2004) 389–397.
[7] C. Giolli, A. Scrivani, G. Rizzi, F. Borgioli, G. Bolelli, L. Lusvarghi, Failure mechanism for thermal fatigue thermal barrier coating systems, Journal of Thermal Spray Technology 18 (2) (2009) 223–230.
[8] M. Bialas, Finite element analysis of stress distribution in thermal barrier coatings, Surface and Coatings Technology 202 (2008) 6002–6010.
[9] M. Ranjbar-Far, J. Absi, G. Mariaux, F. Dubois, Simulation of the effect of material properties and interface roughness on the stress distribution in thermal barrier coatings using finite element method, Materials and Design 31 (2010) 772–781.

[10] P.K. Wright, Influence of cyclic strain on life of a PVD TBC, Materials Science and Engineering A245 (1998) 191–200.
[11] E. Tzimas, H. Muellejans, S.D. Peteves, J. Bressers, W. Stamm, Failure of thermal barrier coating under cyclic thermo-mechanical loading, Acta Materialia 48 (2000) 4699–4707.
[12] M. Okazaki, High-temperature strength of Ni-base super-alloy coatings, Science and Technology of Advanced Materials 2 (2001) 357–366.
[13] B. Baufeld, E. Tzimas, P. Haehner, H. Muellenjans, S.D. Peteves, P. Moretto, Phase-angle effects on damage mechanisms of thermal barrier coatings under thermo-mechanical fatigue, Scripta Materialia 45 (2001) 859–865.
[14] B. Baufeld, E. Tzimas, H. Muellenjans, S. Peteves, J. Bressers, W. Stamm, Thermal-mechanical fatigue of MAR-M 509 with a thermal barrier coating, Materials Science and Engineering A315 (2001) 231–239.
[15] A. Peichl, T. Beck, O. Voehringer, Behavior of an EB-PVD thermal barrier coating system under thermal-mechanical fatigue loading, Surface and Coatings Technology 162 (2003) 113–118.
[16] J. Shi, A.M. Karlsson, B. Baufeld, M. Bartsch, Evolution of surface morphology of thermo-mechanically cycled NiCoCrAlY bond coats, Materials Science and Engineering A434 (2006) 39–52.
[17] A. Aguero, R. Muelas, M. Gutierrez, R.V. Vulpen, S. Osgerby, J. P. Banks, Cyclic oxidation and mechanical behavior of slurry aluminide coatings for steam turbine components, Surface and Coatings Technology 201 (2007) 6253–6260.
[18] K. Rahmani, S. Nategh, Influence of aluminide diffusion coating on low cycle fatigue properties of Rene 80, Materials Science and Engineering A486 (2008) 686–695.
[19] M. Azadi, A. Moridi, G.H. Farrahi, Optimal experiment design for plasma thermal spray parameters at bending loads, International Journal of Surface Science and Engineering 6 (1–2) (2012) 3–14.
[20] X. Zhang, K. Ahmmed, M. Wang, H. Hu, Influence of ageing temperatures and times on mechanical properties of vacuum high pressure die cast aluminum alloy A356, Advanced Materials Research 445 (2012) 277–282.
[21] ASM Handbook, Mechanical Testing and Evaluation, vol. 8, ASM International, Materials Park, OH, USA, 2000.